NASA/TM—2010-216756 AIAA–2010–1127

Numerical Simulation of Vitiation Effects on a Hydrogen-Fueled Dual-Mode Scramjet

Manan A. Vyas
Glenn Research Center, Cleveland, Ohio

William A. Engblom
Embry-Riddle Aeronautical University, Daytona Beach, Florida

Nicholas J. Georgiadis and Charles J. Trefny
Glenn Research Center, Cleveland, Ohio

Vishal A. Bhagwandin
U.S. Army Research Laboratory, Aberdeen Proving Ground, Maryland

July 2010

NASA STI Program . . . in Profile

Since its founding, NASA has been dedicated to the advancement of aeronautics and space science. The NASA Scientific and Technical Information (STI) program plays a key part in helping NASA maintain this important role.

The NASA STI Program operates under the auspices of the Agency Chief Information Officer. It collects, organizes, provides for archiving, and disseminates NASA's STI. The NASA STI program provides access to the NASA Aeronautics and Space Database and its public interface, the NASA Technical Reports Server, thus providing one of the largest collections of aeronautical and space science STI in the world. Results are published in both non-NASA channels and by NASA in the NASA STI Report Series, which includes the following report types:

- TECHNICAL PUBLICATION. Reports of completed research or a major significant phase of research that present the results of NASA programs and include extensive data or theoretical analysis. Includes compilations of significant scientific and technical data and information deemed to be of continuing reference value. NASA counterpart of peer-reviewed formal professional papers but has less stringent limitations on manuscript length and extent of graphic presentations.

- TECHNICAL MEMORANDUM. Scientific and technical findings that are preliminary or of specialized interest, e.g., quick release reports, working papers, and bibliographies that contain minimal annotation. Does not contain extensive analysis.

- CONTRACTOR REPORT. Scientific and technical findings by NASA-sponsored contractors and grantees.

- CONFERENCE PUBLICATION. Collected papers from scientific and technical conferences, symposia, seminars, or other meetings sponsored or cosponsored by NASA.

- SPECIAL PUBLICATION. Scientific, technical, or historical information from NASA programs, projects, and missions, often concerned with subjects having substantial public interest.

- TECHNICAL TRANSLATION. English-language translations of foreign scientific and technical material pertinent to NASA's mission.

Specialized services also include creating custom thesauri, building customized databases, organizing and publishing research results.

For more information about the NASA STI program, see the following:

- Access the NASA STI program home page at *http://www.sti.nasa.gov*

- E-mail your question via the Internet to *help@sti.nasa.gov*

- Fax your question to the NASA STI Help Desk at 443–757–5803

- Telephone the NASA STI Help Desk at 443–757–5802

- Write to:
  NASA Center for AeroSpace Information (CASI)
  7115 Standard Drive
  Hanover, MD 21076–1320

NASA/TM—2010-216756 AIAA–2010–1127

Numerical Simulation of Vitiation Effects on a Hydrogen-Fueled Dual-Mode Scramjet

Manan A. Vyas
Glenn Research Center, Cleveland, Ohio

William A. Engblom
Embry-Riddle Aeronautical University, Daytona Beach, Florida

Nicholas J. Georgiadis and Charles J. Trefny
Glenn Research Center, Cleveland, Ohio

Vishal A. Bhagwandin
U.S. Army Research Laboratory, Aberdeen Proving Ground, Maryland

Prepared for the
48th Aerospace Sciences Meeting
sponsored by the American Institute of Aeronautics and Astronautics
Orlando, Florida, January 4–7, 2010

National Aeronautics and
Space Administration

Glenn Research Center
Cleveland, Ohio 44135

July 2010

Acknowledgments

The authors would like to thank the Test Resource Management Center (TRMC) Test and Evaluation/Science and Technology (T&E/S&T) Program for their support. This work is funded by the T&E/S&T Program through the Advanced Propulsion Test Technology focus area. The authors would also like to thank NASA Fundamental Aeronautics Program's Hypersonics Project for its generous support. The authors wish to thank Dr. Christopher Goyne and Dr. Robert Rockwell at the University of Virginia for providing experimental data, Embry-Riddle Aeronautical University for providing supercomputer resources, and the NPARC Alliance for providing Wind-US technical support.

Level of Review: This material has been technically reviewed by technical management.

Available from

NASA Center for Aerospace Information
7115 Standard Drive
Hanover, MD 21076–1320

National Technical Information Service
5301 Shawnee Road
Alexandria, VA 22312

Available electronically at http://gltrs.grc.nasa.gov

Numerical Simulation of Vitiation Effects on a Hydrogen-Fueled Dual-Mode Scramjet

Manan A. Vyas
National Aeronautics and Space Administration
Glenn Research Center
Cleveland, Ohio 44135

William A. Engblom
Embry-Riddle Aeronautical University
Daytona Beach, Florida 32114

Nicholas J. Georgiadis and Charles J. Trefny
National Aeronautics and Space Administration
Glenn Research Center
Cleveland, Ohio 44135

Vishal A. Bhagwandin
U.S. Army Research Laboratory
Aberdeen Proving Ground, Maryland 21005

Abstract

The Wind-US computational fluid dynamics (CFD) flow solver was used to simulate dual-mode direct-connect ramjet/scramjet engine flowpath tests conducted in the University of Virginia (UVa) Supersonic Combustion Facility (SCF). The objective was to develop a computational capability within Wind-US to aid current hypersonic research and provide insight to flow as well as chemistry details that are not resolved by instruments available. Computational results are compared with experimental data to validate the accuracy of the numerical modeling. These results include two fuel-off non-reacting and eight fuel-on reacting cases with different equivalence ratios, split between one set with a clean (non-vitiated) air supply and the other set with a vitiated air supply (12 percent H_2O vapor). The Peters and Rogg hydrogen-air chemical kinetics model was selected for the scramjet simulations. A limited sensitivity study was done to investigate the choice of turbulence model and inviscid flux scheme and led to the selection of the k-ε model and Harten, Lax and van Leer (for contact waves) (HLLC) scheme for general use. Simulation results show reasonably good agreement with experimental data and the overall vitiation effects were captured.

Nomenclature

C_f, C_b	forward and backward reaction rate coefficients
C_μ	turbulent viscosity coefficient
D_f, D_b	forward and backward reaction rate energies
D	mass diffusivity
H	compression ramp height at the fuel injection location
K_b	Boltzmann constant
k	turbulent kinetic energy
M	Mach number
$\dot{m}_a, \dot{m}_f$	Air and fuel mass flow rates
P_o, P	stagnation and static pressure

P_{ref}	reference pressure at isolator entrance
Pr_l, Pr_t	laminar and turbulent Prandtl number
Sc_l, Sc_t	laminar and turbulent Schmidt number
S_f, S_b	forward and backward reaction rate exponent
T_o, T	stagnation and static temperature
α	thermal diffusivity
μ	dynamic viscosity
ν	kinematic viscosity
Φ_{EXP}, Φ_{CFD}	experimental and numerical fuel-equivalence ratio

I. Introduction

Significant progress has been made in hypersonic research and scramjet technology in recent years, mostly in the areas of vehicle design and propulsion. Now that hypersonic research and development programs are testing and refining their designs, there is a general need for efficient, safe and cost-effective tools to aid the development of these vehicles. Numerical simulation is one approach to aid experimental tests, perform parametric studies and check if design changes are worth testing experimentally. It also provides important insight into complex flow phenomena like separations, shockwave boundary layer interactions, mode transition, and turbulence-chemistry interactions, thus significantly improving the flowpath design process for relatively lower costs compared to costly experimental tests alone. One such tool is Wind-US, a computational fluid dynamics (CFD) platform developed by the NPARC Alliance, a partnership between NASA Glenn Research Center (GRC), USAF Arnold Engineering & Development Center (AEDC), and Boeing Phantom Works. Wind-US is a general-purpose Reynolds-averaged Navier-Stokes (RANS) flow solver that supports equation sets governing turbulent and chemically reacting, compressible flows (Refs. 1 and 2). It has a set of pre- and post-processing utilities that helps in analyzing a case from start to finish.

The validation of Wind-US for scramjet applications was a primary objective of this research work. The scope of current research included simulating a dual-mode direct-connect ramjet/scramjet engine flowpath using Wind-US. Results obtained from the simulations are compared with the experimental data from the UVa Supersonic Combustion Facility (SCF). Comparisons are made in terms of static pressures along the centerline of the experimental facility. Numerical simulations are performed for a set of experimental run conditions (referred to as *scans* in reference to specific experimental measurements), which include a range of fuel-equivalence ratios within the mode transition regime, i.e., transition from supersonic to subsonic combustion. In addition, the effects of H_2O flow vitiation on the combustion process and thus the mode transition was also investigated. This is largely motivated by the fact that large experimental tunnel facilities burn fuel to heat supply air for matching the flight conditions, i.e., enthalpies and stagnation temperature. Burning of the fuel can add H_2O and CO_2 vitiates to the flow entering the combustion chamber. However, the smaller UVa SCF uses an electric heater to heat the supply air for matching the flight conditions. As a result, for the vitiated air experimental runs, H_2O and CO_2 vitiates could be added to the air stream from a separate supply rather than a combustion process in order to replicate the situation of larger facilities. This research work only focused on H_2O vitiate cases.

The results and experience of the current work should contribute to the validation of Wind-US for hypersonic propulsion applications. To accomplish this, the study attempted to provide results as well as the procedure required to obtain the results in order to help other hypersonics researchers make the best choice of chemical kinetics, numerical scheme, turbulence model and various other choices associated with the CFD simulation of combusting flow.

II. Background

Some previous work on simulating a ramjet/scramjet flowpath was done by Baurle and Eklund (Ref. 3) on the US AFRL/Aerospace Propulsion Laboratory scramjet combustor. The entire flowpath was modeled using the VULCAN RANS flow solver to perform a Schmidt number and grid sensitivity study. The focus of the study was to understand the precombustion shock train, flameholding, and turbulent mass and heat transfer characteristics. Another such study was performed by Goyne et al. (Ref. 4) where individual components of the UVa dual-mode direct-connect ramjet/scramjet flowpath were also simulated using VULCAN. The results concluded that the turbulent mixing as well as the levels of heat release of combustion are under-predicted. Engblom et al. (Ref. 5) successfully simulated a direct-connect ramjet/scramjet flowpath derived from X-43B using Wind-US. A study preceding the current work was done by Bhagwandin et al. (Ref. 6) where the UVa dual-mode direct-connect ramjet/scramjet flowpath was simulated in its entirety. The study focused on limited fuel-equivalence ratios as the primary goal was investigating various finite-rate chemistry models and overall successful simulation of UVa flowpath. Present work expands on the knowledge of previous work and examines fuel equivalence ratios corresponding to mode transition and the effects of flow vitiation.

Mode transition is a process that starts with a ramjet mode and evolves into a scramjet mode. In a ramjet the combustor operates at subsonic speeds, i.e., a subsonic combustion process (Ref. 7). This means that the isolator, which precedes the combustor, slows the flow down via a series of shocks ending with a normal shock to deliver a subsonic flow to the combustor. The hybrid shock structure is comprised of lambda and normal shocks, which also produce large boundary layer separations. As the vehicle flight speed increases from the ramjet envelope (Mach 2-5) to the scramjet envelope (Mach 5-20), the loss in total pressure associated with diffusing inlet airflow to subsonic speeds for combustion becomes very large, lowering the performance of the dual-mode engine. Thus, it becomes necessary to carry out the fuel-air mixing and combustion process at supersonic speeds, transitioning the engine to scramjet operation. The transition from ramjet to scramjet mode occurs as the flight speed increases which brings the total temperature ratio across the combustor down, effectively reducing the pressure rise in the combustor (Ref. 8). The reduced combustor pressures decrease the shock train strength, eliminating the terminal normal shock to the combustor entrance giving way to the supersonic combustion. The boundary layer separation decreases as a result of a weaker shock train. Additionally, adjustments made to the fuel-equivalence ratio results in the shock train being entirely swallowed by the combustor, resulting in scramjet mode. However, in the UVa facility, the mode transition is achieved by throttling the fuel supply to the combustor.

Finite-rate chemistry modeling is one of the most important aspects of the ramjet/scramjet flowpath simulation. A variety of multi-reaction chemistry models exist for use in simulations of reacting flow in a ramjet/scramjet combustor. Generally speaking, the more detailed the reaction set the better the accuracy expected of a model to simulate the highly complex and unsteady nature of the combustion process. In the study performed by Engblom et al. (Ref. 5), a 7-species, 3-reaction as well as a 5-species, 1-reaction ethylene-air kinetics model were used. The former gave a better prediction of heat release and thus the flow characteristics. Particular to the present research were various hydrogen-air chemistry models. One such model investigated by Goyne et al. (Ref. 4) was a 7-species, 7-reaction mechanism, however it was unable to simulate flame holding and thus was replaced by a simpler 4-species, 1-reaction mechanism.

In the previous efforts to simulate UVa's dual-mode direct-connect flowpath, Georgiadis et al. (Ref. 9) used a 1-reaction mechanism and Bhagwandin et al. (Ref. 6) used a 7-species, 8-reaction Evans and Schexnayder (Ref. 10) mechanism, modified to include third-body efficiencies. However, for the current work a 9-species, 18-reaction, Peters and Rogg (Ref. 11) chemistry model is used. The primary motivation behind using Peters and Rogg is the fact that it is a nearly complete H-O reaction set. It includes 18 out of 20 possible H-O reactions (Ref. 12) reactions making it a comprehensive hydrogen-air chemistry model, which is essential to investigate vitiated air effects on the mode transition behavior. The model also includes species-dependent third-body efficiencies of 3 species.

Turbulence-chemistry interactions have a considerable effect on the species production rates in the chemically reacting flows (Refs. 13 to 16). Even though several CFD solvers have the capability of simulating chemically reacting flows, most turbulence models are only capable of representing turbulent effects of the momentum transport in the flow field, thus ignoring the fluctuations in the species production rates and disregarding the turbulence-chemistry interactions. Essentially speaking the turbulence is decoupled from the chemical kinetics. The usual practice is to then employ a constant Sc_t and Pr_t number or the ratio of the previous to latter called the Lewis number. Sc_t is the ratio of momentum diffusivity to mass diffusivity, Equation (1). Thus, Sc_t dictates the turbulent mixing behavior of the various species.

$$Sc_t = \frac{\nu}{D} = \frac{\mu}{\rho D} = \frac{\text{momentum diffusivity}}{\text{mass diffusivity}} \tag{1}$$

A high value of Sc_t results in reduced mixing, and possible flameout while a low value of Sc_t results in mixing that is too fast, elevating the pressures in the combustor and producing a shock train which reaches the inlet causing an unstart. Pr_t is defined as the ratio of momentum eddy diffusivity to thermal eddy diffusivity, and is used to quantify the heat flux or temperature fluctuations in the flow field caused by turbulent transport.

$$Pr_t = \frac{\nu}{\alpha} = \frac{\mu}{\rho\alpha} = \frac{\text{momentum diffusivity}}{\text{thermal diffusivity}} \tag{2}$$

A study of Pr_t sensitivity was done by Engblom et al. (Ref. 5) and Keistler et al. (Ref. 13). Both similarly demonstrated that the effect of decreasing Pr_t was reduced reaction rates and delayed ignition. However, this sensitivity to Pr_t was limited. It is expected that Sc_t has a greater effect on ignition and subsequent combustion behavior because it has a higher influence on increasing the concentration of reactants needed to move a chemical reaction forward.

For the purpose of the current work a constant Sc_t and Pr_t number are assumed. Variable Sc_t and Pr_t models are currently in development and may result in improved prediction of scramjets in the future, but are not considered ready for realistic scramjet simulations at the time of this work. Efforts have been undertaken by Xiao et al. (Ref. 16) and Keistler et al. (Ref. 13) to model scramjet flows with variable Sc_t and Pr_t models. The results obtained by Xiao et al. (Ref. 16) showed a promising capability in predicting chemically reacting flows. The results also showed that the use of a multi-variate β-Probability Density Function (PDF) is highly dissipative which results in reduced mixing and ineffective capturing of the turbulence-chemistry interactions.

III. Experimental Configuration

Experimental data acquired at the UVa SCF was used for comparison with the numerical flow simulations performed in the current work. The direct-connect facility is vertically mounted and has dual-mode direct-connect capabilities. Figure 1 shows the supply nozzle, isolator, combustor, extender, fuel lines, coolant lines and numerous pressure transducers as well as thermocouples.

As discussed earlier, the facility has a unique ability to provide clean as well as vitiated airflow. The supply nozzle is connected to a 300 kW, 14-stage electrical resistance heater, fed by the oil-free compressor, which accomplishes air heating (Ref. 4) to match flight conditions and is capable of delivering a clean vitiate-free airflow of about 1200 K for the clean air experiments. However, in order to provide the vitiated airflow, H_2O was added to the airflow from an external source. In an effort to precisely match the conditions in the large tunnels, make-up oxygen was also added to the airflow to obtain 21 percent O_2.

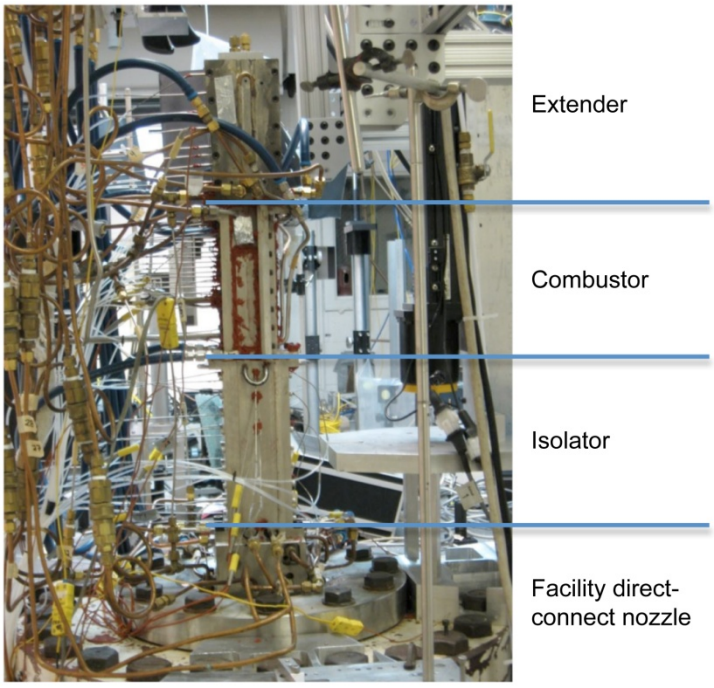

Figure 1.—UVa Supersonic Combustion Facility (Ref. 17).

The convergent-divergent supply nozzle delivers a Mach 2 flow to the constant-area isolator. This direct-connect nozzle is used to replicate the flow that an inlet would provide to the isolator in an actual flight. The isolator ends where the fuel-injector ramp begins. The isolator and combustor have a cross-sectional area of 1.5×1.0 in.^{2}. The compression ramp has an angle of 10° and a base height (H) of 0.25 in. The dimensions in Figure 2 are normalized using this base height. Immediately after the combustor follows the 2.9° diverging extender-nozzle. At the exit of the extender-nozzle the airflow is exhausted to the ambient atmosphere. The exhaust plume is captured by a catch-cone, which directs the exhaust gases vertically out of the building.

Hydrogen fuel is injected in the core flow at the base of the compression ramp using a Mach 1.7 conical nozzle. Once the fuel injection reaches a steady-state, it is ignited using a detonation-driven igniter system. Combustion is self-sustaining once ignited.

One of the challenging aspects of simulating the UVa SCF flowpath is properly modeling the thermal boundary conditions. The facility is fabricated with various metals and a sophisticated cooling channel topology. These metals and cooling channel patterns differ within the three major sections (isolator, combustor, and extender-nozzle), making it an extremely difficult problem from the numerical simulation point of view.

Figure 3 shows the metals used in the fabrication, cooling channels, and window locations on each wall of the facility. The supply nozzle, isolator and extender-nozzle are all made with Nickel 200. However, the inner isolator walls are coated with 0.4 mm zirconia coating. The north and south walls have side windows that do not span the entire width of the wall in the combustor. The west wall is the fuel injector wall. The fuel injector wall of the combustor section is made with Nickel 200, unlike the other three walls, and coated with zirconia to protect the inner wall from high temperatures. It also has internal parallel cooling channels. The east wall is opposite to the fuel injector wall. Here, an observation window spans the entire width of the wall. All windows have a ceramic blank insert. The black bold line shows the flowpath perimeter for each face while the solid black lines are external cooling channels and dotted lines are embedded in the wall. The arrows show the direction of flow through the cooling channels. The orange channels in the combustor section represent the cooling channels located in the corners but they are not directly part of the wall. To summarize, the effects of internal versus external

Nozzle, x		Coordinates, y	
0.000	1.580	1.120	1.328
0.408	2.108	1.132	1.448
0.572	2.996	1.148	1.624
0.652	3.784	1.156	1.752
0.720	4.812	1.164	1.872
0.808	5.684	1.176	1.940
0.956	6.484	1.196	1.980
1.084	7.074	1.220	1.996
1.316	7.872	1.268	2.000
	7.880		2.000

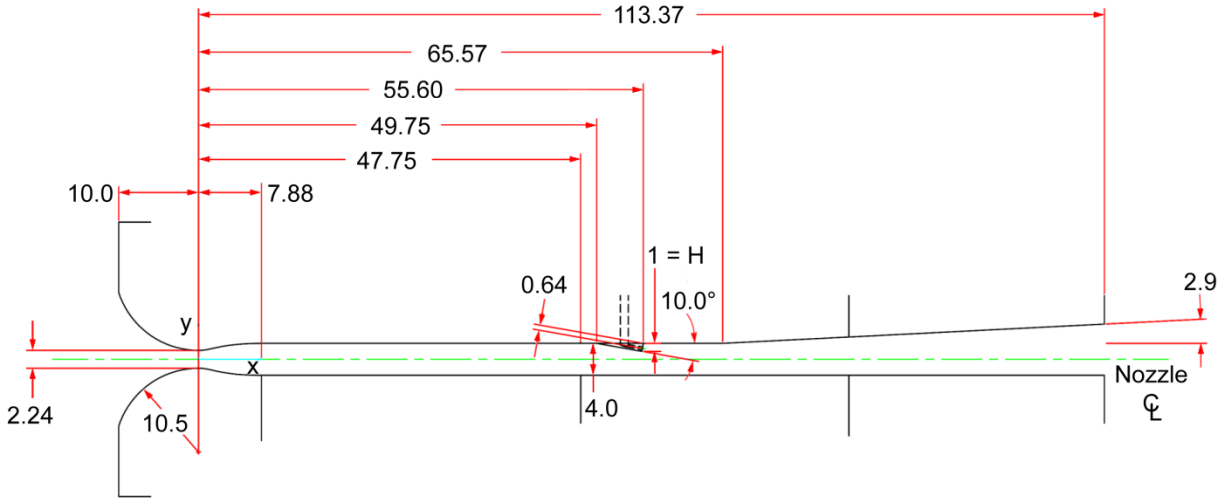

Figure 2.—UVa flowpath schematic (Ref. 17).

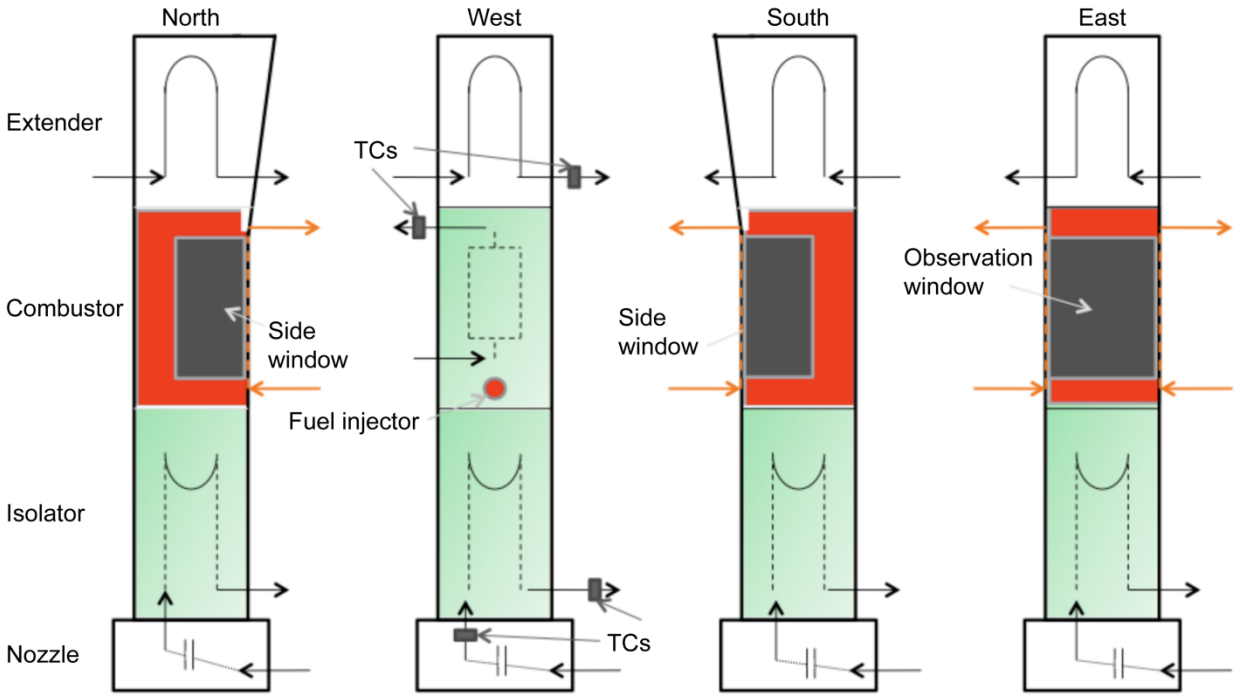

• Dashed lines are interior channels, solid lines are exterior tubes, breaks denote uncertain physical routing.
• White = nickel 200, Red = 304 stainless steel, Green = zirconia coating on nickel 200, Black = ceramic blanks.

Figure 3.—Facility fabrication, cooling channels and windows (Ref. 17).

cooling channels, heat transfer through nickel versus stainless steel versus zirconia coated surfaces, wall-cooling channels versus the corner cooling channels and the presence of the ceramic blanks adds a considerable uncertainty in the experimental thermal data, especially in the combustor and extender-nozzle, and make for a challenging comparison with the results of the current numerical simulation.

IV. Methodology

A. Computational Mesh

Several computational grids were examined during the course of simulations with Wind-US. Significant efforts were undertaken to apply sufficient grid resolution in the areas of interest, namely the isolator, isolator-ramp, combustor, and fuel injector in order to resolve the key flow features.

For the purpose of this work, a three-dimensional, structured grid was created for the UVa dual-mode direct-connect flowpath, shown in Figure 4. Symmetry was used to model one half of the flowpath with the symmetry plane being the central ($z = 0$) plane. The colored planes in Figure 4 denote the plane of symmetry. The final mesh contains 5.82 million structured grid points split into 39 zones for parallel processing. In order to better resolve the turbulence and the fuel-air shear layer mixing, the combustor zones adjacent to the fuel injection were mismatched with the adjacent zones. A mismatch or a non point-to-point match between two zonal boundaries allowed for a denser grid in the area of interest and coarser grid away from it.

Lastly, care was taken to ensure proper wall packing was maintained throughout the entire flowpath to better capture shock boundary layer interactions and boundary layer separations. The resulting grid had a nominal y^+ of below 5, which was deemed sufficient to model wall boundary layer effects in these numerical simulations.

B. Flow Conditions

For the purpose of this research work, a total of ten cases were identified for numerical simulation (see Table 1) with the objective of investigating the fuel equivalence ratios corresponding to the mode transition regime for clean as well as vitiated air. The fuel-off cases were also simulated with clean and vitiated air to verify the data in absence of the combustion. The vitiated air cases were examined to better understand the flow vitiate effects on combustion process.

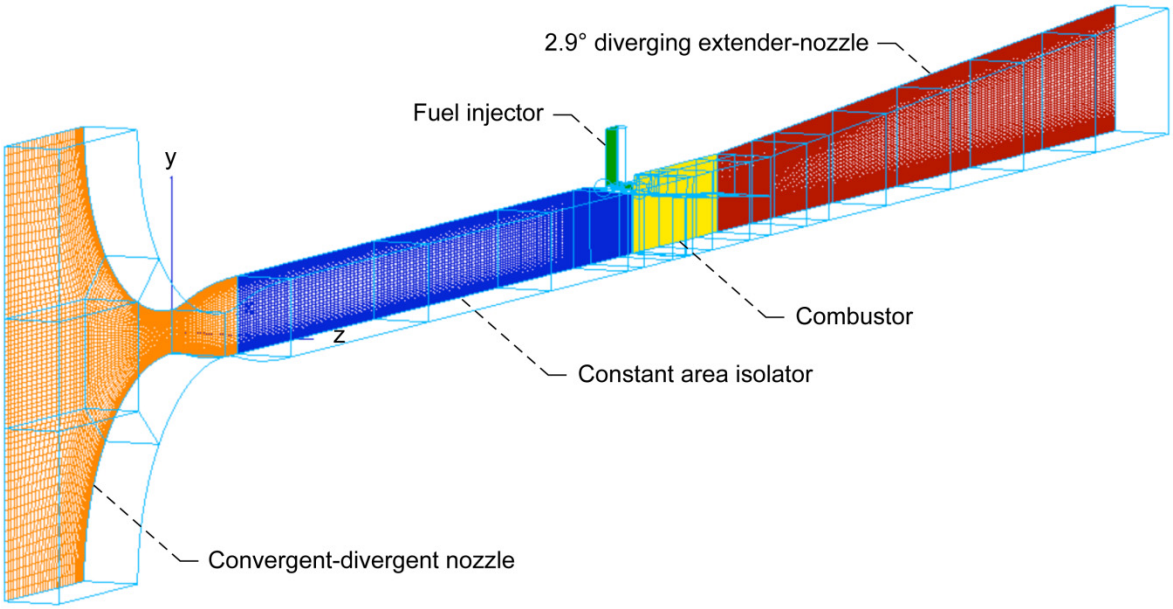

Figure 4.—Three-dimensional structured mesh.

TABLE 1.—UVa TEST CASES

Cases	Equivalence ratio	Stagnation conditions	H_2 Fuel plenum conditions	Ambient conditions
Clean air				
Scan 1	0.000	*Po* = 327.72 kPa *To* = 1201 K $\dot{m}_a$ = 0.202 kg/s	----------	Patm = 99.1 kPa Tatm = 294.4 K
Scan 4	0.172	*Po* = 326.97 kPa *To* = 1202 K $\dot{m}_a$ = 0.201 kg/s	*Po* = 527.14 kPa *To* = 298.86 K $\dot{m}_f$ = 1.01E-3 kg/s	Patm = 99.1 kPa Tatm = 294.4 K
Scan 14	0.260	*Po* = 327.20 kPa *To* = 1202 K $\dot{m}_a$ = 0.201 kg/s	*Po* = 709.94 kPa *To* = 298.96 K $\dot{m}_f$ = 1.54E-3 kg/s	Patm = 99.1 kPa Tatm = 294.4 K
Scan 5	0.341	*Po* = 327.12 kPa *To* = 1202 K $\dot{m}_a$ = 0.201 kg/s	*Po* = 1042.70 kPa *To* = 299.32 K $\dot{m}_f$ = 2.01E-3 kg/s	Patm = 99.1 kPa Tatm = 294.4 K
Scan 9	0.454	*Po* = 327.07 kPa *To* = 1202 K $\dot{m}_a$ = 0.201 kg/s	*Po* = 1394.04 kPa *To* = 299.74 K $\dot{m}_f$ = 2.66E-3 kg/s	Patm = 99.1 kPa Tatm = 294.4 K
12% H_2O vitiate air				
Scan 35 (11% H_2O)	0.000	*Po* = 329.56 kPa *To* = 1203 K $\dot{m}_a$ = 0.198 kg/s	----------	Patm = 98.9 kPa Tatm = 294.4 K
Scan 28	0.175	*Po* = 326.80 kPa *To* = 1204 K $\dot{m}_a$ = 0.196 kg/s	*Po* = 548.55 kPa *To* = 297.80 K $\dot{m}_f$ = 1.04E-3 kg/s	Patm = 99.1 kPa Tatm = 294.4 K
Scan 18	0.267	*Po* = 326.87 kPa *To* = 1203 K $\dot{m}_a$ = 0.196 kg/s	*Po* = 829.67 kPa *To* = 298.64 K $\dot{m}_f$ = 1.59E-3 kg/s	Patm = 99.1 kPa Tatm = 294.4 K
Scan 23	0.349	*Po* = 326.95 kPa *To* = 1204 K $\dot{m}_a$ = 0.196 kg/s	*Po* = 1092.27 kPa *To* = 297.75 K $\dot{m}_f$ = 2.08E-3 kg/s	Patm = 99.1 kPa Tatm = 294.4 K
Scan 22	0.460	*Po* = 326.88 kPa *To* = 1203 K $\dot{m}_a$ = 0.196 kg/s	*Po* = 1447.78 kPa *To* = 298.55 K $\dot{m}_f$ = 2.75E-3 kg/s	Patm = 99.1 kPa Tatm = 294.4 K

C. Boundary Conditions

As discussed in Section III, the facility components were made of different materials and some surfaces were coated while others were simply ceramic blanks. This, in addition to the various cooling channels made the choice of appropriate thermal boundary conditions a challenge.

A lack of thermocouple data in key components like the combustor and extender-nozzle made the choice of accurate wall temperatures difficult to determine. The combustor is certainly one of the key components considered in this numerical simulation. The combustion process provided a large temperature gradient axially along the flowpath and along the height of the flowpath. This means that the heat transfer profile on the fuel injector wall, the location where thermocouple wells are drilled and cooling channels exist is significantly different than the wall opposite to the fuel injector. The remaining walls in the combustor are ceramic blanks and 304 stainless steel with no cooling channels. Thus, based on the available information any choice of a single wall temperature will be far from an accurate representation of the entire combustor component. To investigate effect of the wall temperature a variety of simulations were performed and the results showed a significant effect on the peak combustion pressure and length and location of the shock train. However, due to Wind-US limitations and to facilitate the research work a representative average wall temperature of 1000 K in the combustor section was used.

This was an average of thermocouple data obtained from the fuel injector wall and typical temperature observed in numerical simulations when the combustor walls were set to adiabatic condition. A choice of constant temperature was also made for the supply nozzle, isolator and extender-nozzle based on the available thermocouple data.

D. Numerics

The Roe second-order upwind-biased flux-difference splitting scheme (Ref. 18), modified for stretched grids was the initial choice for the present simulations, however early results using the Roe scheme were not found to be consistent in predicting the flow separation in the isolator. The predicted numerical separation would switch walls depending on how the solution was initialized. This predicted flow separation behavior was very sensitive to the choice of overall parameters and a small change would cause the switch to occur. Thus, an alternate numerical scheme was examined.

The HLLC scheme due to Harten, Lax and van Leer (for contact waves) (Ref. 19), which is also available within Wind-US, was the next choice based on past experience and other successful simulations. HLLC was found to be much more consistent in predicting the flow separation behavior, and thus it was chosen for all subsequent numerical simulations. The minmod Total Variation Diminishing (TVD) limiter was also used in conjunction with the HLLC numerical scheme. As the name suggests it prevents overshoots in the flow properties in the areas having steep gradients like the combustor and shocks.

Local time stepping with a constant Courant Friedrichs Lewy (CFL) number was used to advance the solution to a steady-state. Thus the solution advances at different rates in various parts of the computational domain. Care was taken to identify a converged steady-state solution by comparing solutions at various times in the non-dimensional time advancement. Various key parameters were monitored to determine the convergence; namely 1) the residuals of Navier-Stokes equations, 2) water mass flux at the exit plane, which is a key indicator of combustion characteristics, 3) the net mass flux, and 4) pressure along the symmetry plane of the fuel injector wall.

E. Turbulence and Chemistry Modeling

The Chien k-ε (Ref. 20) and the Shear Stress Transport (SST) (Ref. 21) turbulence models were initially picked for evaluation. Based on the results obtained for the fuel-off and preliminary calculations for fuel-on (i.e., $\Phi_{EXP} = 0.341$) case, the Chien k-ε model was picked for the scramjet simulations. It is well known that the k-ε model is prone to over-prediction of skin friction drag in flow with adverse pressure gradients and diffusers. To help overcome this issue, the variable C_μ option of the k-ε model (Ref. 22) was used to reduce turbulent viscosity in the flow field where production of turbulent kinetic energy is much higher than the rate of dissipation. Based on some preliminary investigation a choice of baseline constant Sc_t of 0.6 and Pr_t of 0.9 were made for all simulations.

The 13-species, 27-reaction Peters & Rogg (Ref. 11) chemical kinetics model was selected and first validated using the Burrows-Kurkov (Ref. 23) supersonic combustion benchmark case. The benchmark case was validated using two versions of the chemistry model, 1) full 13-species, 27-reaction set and 2) 9-species, 18-reaction set. Since CO_2 was not a vitiate used for cases examined in this work, carbon species were removed from the model (1) to obtain a subset model (2). The validation showed identical results for both versions of the model as expected. However, the subset model provided a significant speed-up in the computations because the additional species equations were not being solved. Thus, the subset model was used for the remaining UVa flowpath simulations. Table 2 shows the subset chemistry model. It should be noted that the UVa experiments (Ref. 17) did make measurements of vitiated air runs including CO_2 vitiates.

TABLE 2.—9-SPECIES, 18-REACTIONS PETERS AND ROGG CHEMISTRY MODEL (REF. 34)

Reaction	S_f S_b	D_f/K_B D_b/K_B, K	C_f C_b, cm^3/mole-sec
$H_2 + O_2 \Leftrightarrow 2OH$	0.0 0.0	2.4230E+04 0.0	1.70E+13 0.0
$H + O_2 \Leftrightarrow OH + O$	0.0 0.0	0.8455E+04 0.0	2.00+14 0.0
$H_2 + OH \Leftrightarrow H_2O + H$	1.6 0.0	1.6608E+03 0.0	1.00E+08 0.0
$H_2 + O \Leftrightarrow OH + H$	2.67 0.0	3.1631E+03 0.0	5.06E+04 0.0
$OH + OH \Leftrightarrow O + H_2O$	1.14 0.0	0.5033E+02 0.0	1.50E+09 0.0
$H + OH + M^a \Leftrightarrow H_2O + M^a$	–2.0 0.0	0.0 0.0	2.22E+22 0.0
$H + H + M^a \Leftrightarrow H_2 + M^a$	–1.0 0.0	0.0 0.0	1.80E+18 0.0
$H + O_2 + M^a \Leftrightarrow HO_2 + M^a$	–0.8 0.0	0.0 0.0	2.30E+18 0.0
$HO_2 + OH \Leftrightarrow H_2O + O_2$	0.0 0.0	0.0 0.0	6.00E+13 0.0
$HO_2 + H \Leftrightarrow H_2 + O_2$	0.0 0.0	352.3 0.0	2.53E+13 0.0
$HO_2 + H \Leftrightarrow OH + OH$	0.0 0.0	505.28 0.0	1.50E+14 0.0
$HO_2 + O \Leftrightarrow OH + O_2$	0.0 0.0	–203.8 0.0	1.80E+13 0.0
$O + O + M^a \Leftrightarrow O_2 + M^a$	–1.0 0.0	0.0 0.0	2.90E+17 0.0
$HO_2 + H \Leftrightarrow H_2O + O$	0.0 0.0	865.63 0.0	3.00E+13 0.0
$HO_2 + HO_2 \Leftrightarrow H_2O_2 + O_2$	0.0 0.0	–626.57 0.0	2.50E+11 0.0
$OH + OH + M^a \Leftrightarrow H_2O_2 + M^a$	–2.0 0.0	0.0 0.0	3.25E+22 0.0
$H_2O_2 + H \Leftrightarrow H_2O + OH$	0.0 0.0	1804.2 0.0	1.00E+13 0.0
$H_2O_2 + OH \Leftrightarrow H_2O + HO_2$	0.0 0.0	505.28 0.0	5.40E+12 0.0

[a]The third-body efficiencies are H_2O: 6.5, O_2: 0.4, N_2: 0.4.

V. Results

A. Φ_{EXP} = 0.000 (Fuel-Off)

The boundary conditions for the fuel-off case were modified in order to account for lack of fuel flow in the injector. The entrance to the fuel injector is sealed off and replaced with a viscous wall. No calculations were performed in the fuel injector zones.

A turbulence model sensitivity study is performed in order to find a suitable model for the flowpath simulations. The results are compared with that of the experiment in Figure 5 and show a good match between numerical and experimental pressure distributions when the *k*-ε turbulence model is used. The simulation was not capable of picking up small pressure fluctuations in the isolator from x/H = –45 to –10, however the pressure estimates stayed within the range. The pressure peak caused by the fuel injector ramp at x/H = –5 matches very well with the experiment. The peak pressure in the combustor is over-predicted but overall *k*-ε results in the combustor and extender-nozzle matched well with that of the experiment. The SST model was unable to predict the flow behavior from x/H = 25 to 40. This was somewhat surprising because the SST model usually provides better predictions of separated flows than *k*-ε in benchmark validation exercises.

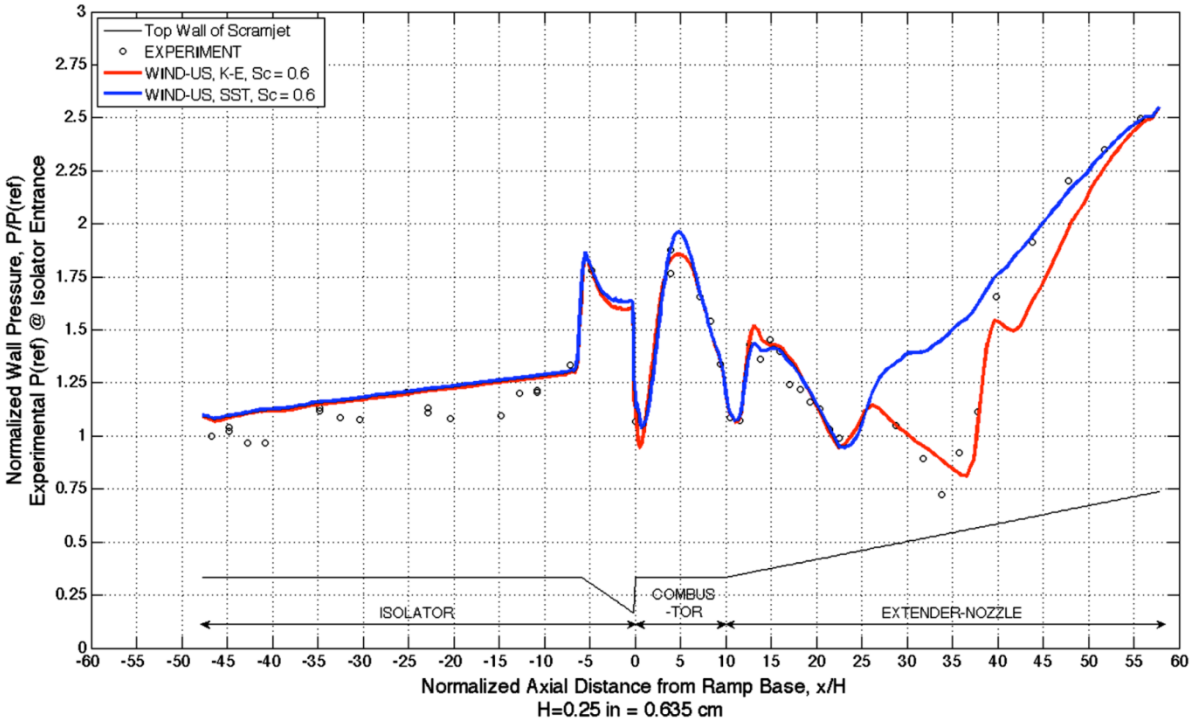

Figure 5.—Pressure along the fuel injector wall at symmetry plane, Φ_{EXP} = 0.000 (fuel-off), *k*-ε versus SST.

The shock produced by the compression ramp propagates downstream to the combustor and the extender-nozzle. These shock structures cause the peaks and valleys in the pressure profile. Figure 7 shows the core flow through the combustor, and the extender-nozzle remains supersonic in the absence of the combustion. There is also the presence of a recirculation region in the combustor immediately aft of the compression ramp. As the flow enters the extender-nozzle and turns the 2.9° expansion corner it further accelerates and reaches nearly Mach 2. At x/H = 40 the flow shows signs of separation but does not separate until x/H = 50. This phenomenon is also evident from Figure 5. This eventually leads to a modest discrepancy between numerical and experimental pressures at the exit of the extender-nozzle. This could be attributed to the *k*-ε turbulence model as it is well known for over-predicting skin friction in wall boundary layers that have adverse pressure gradients and experimentally tend to separate (Ref. 22). However, the agreement with experimental data is still surprisingly much better than that provided by the SST model. Based on the turbulence model sensitivity study, the *k*-ε model was chosen for remainder of the mode transition and vitiation effects investigation.

Figure 6 shows a comparison between the clean and H_2O vitiated air with that of the experimental data. The numerical simulation provides a good match to the experimental data. However, at the beginning of the isolator, it may be observed that the normalized clean air numerical result is approximately 8 percent higher than the vitiated air. This modest discrepancy is observed for other fuel-equivalence ratios as well. The experimental reference pressure, P_{ref} (measured at the beginning of the isolator) for each *scan* is used to normalize all numerical result, and is the source of this discrepancy. For the same inflow conditions (i.e., upstream stagnation pressure and temperature) the experiments indicated that the clean air reference pressure was nearly 8 percent lower than 12 percent H_2O vitiated air, while the computations indicated approximately 1.5 percent lower pressure for the clean air cases. A subsequent one-dimensional analysis of the nozzle indicated an expected difference close to the Wind-US prediction. Also, the experimental reference pressure is within 2 percent of one-dimensional analysis and the Wind-US prediction for vitiated air, however, it is within 8 percent of one-dimensional analysis and the Wind-US prediction for the clean air. Further investigation is needed to determine the source of this discrepancy between experimental, one-dimensional analysis and Wind-US predictions for clean air cases.

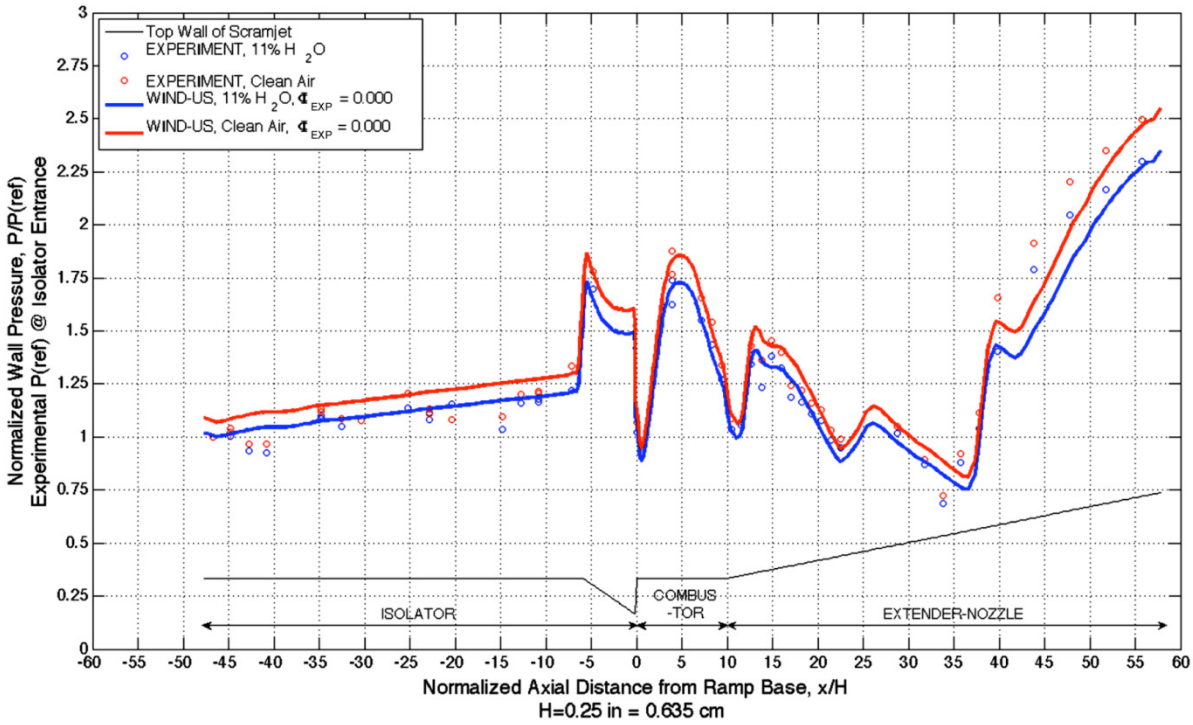

Figure 6.—Pressure along the fuel injector wall at symmetry plane, Φ_{EXP} = 0.000 (fuel-off).

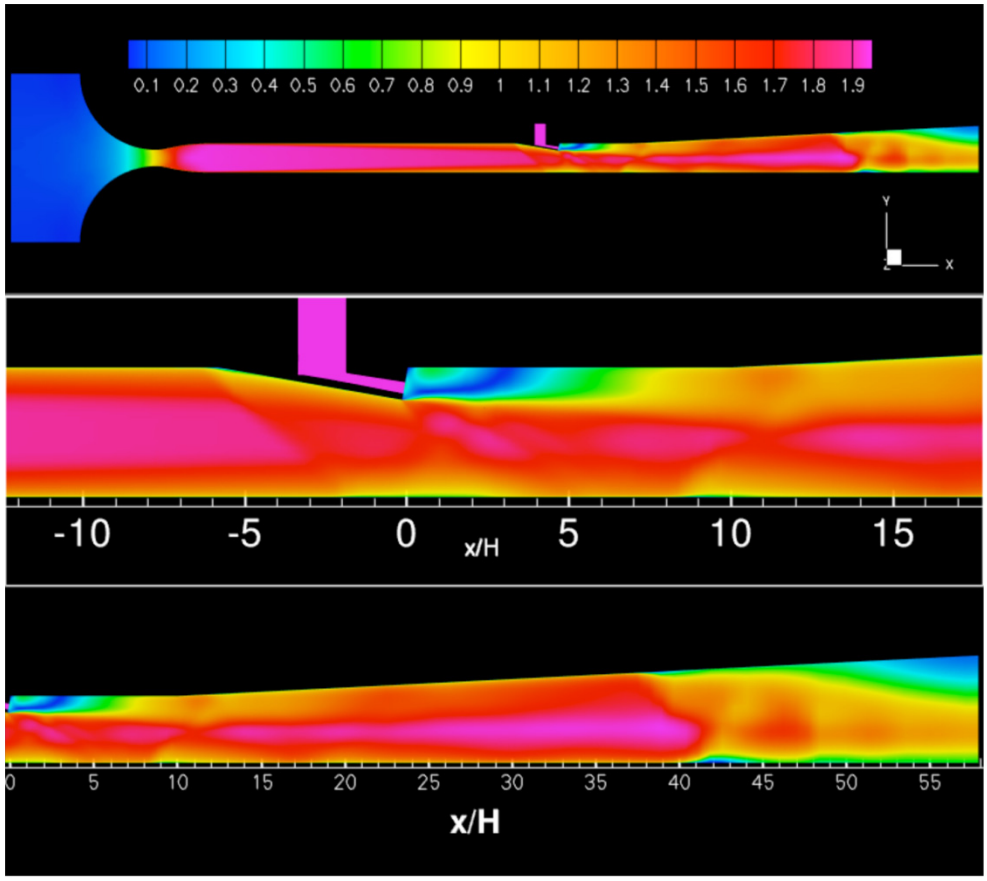

Figure 7.—Mach number contours at the symmetry plane, Φ_{EXP} = 0.000 (fuel-off), *k*-ε.

B. $\Phi_{EXP} \approx 0.170$

Figure 8 shows a comparison of numerical results for $\Phi_{EXP} = 0.172$ (clean air) and 0.175 (vitiated air) with that of experimental data. Both the experimental data and the numerical results show a subtle reduction in the peak pressures in the combustor and overall reduced pressures in the isolator and extender-nozzle when 12 percent H_2O is added to the supply nozzle airflow. While the numerical results show good qualitative agreement in the isolator, a choice of $Sc_t = 0.6$ did not provide a good prediction of the combustor pressure distribution for either case. The pressures are under-predicted in the combustor as well as in the extender-nozzle. The numerical simulation also failed to predict a rapid drop in pressure at x/H = 25, which becomes less evident for high fuel-equivalence ratios. The constant Sc_t model likely causes a quick mixing of fuel-air resulting in abrupt combustion. A variable Sc_t model would better represent the turbulent effects of the species fluctuation, and could in turn potentially better represent the fuel-air mixing over the length of the combustor and the increased pressures due to the combustion process.

Since the qualitative behavior of the flow is similar for both cases, Figure 9 shows the Mach number contours for the $\Phi_{EXP} = 0.172$ (clean air). It is evident that the first shock is caused by the compression ramp at x/H = –5. The shock reflections propagate downstream to the combustor, however the majority of the flow entering the combustor is supersonic, thus the combustor is operational in scramjet mode.

The flow separation in the extender-nozzle occurs at x/H = 30 in the numerical results while the experiment shows a flow separation at x/H = 40. This could be due to a combined effect of limitation in the turbulence model, the constant Sc_t model, which does not account for turbulence-chemistry interactions, and/or the temperature boundary conditions used. Further analysis is needed to identify the cause of this behavior.

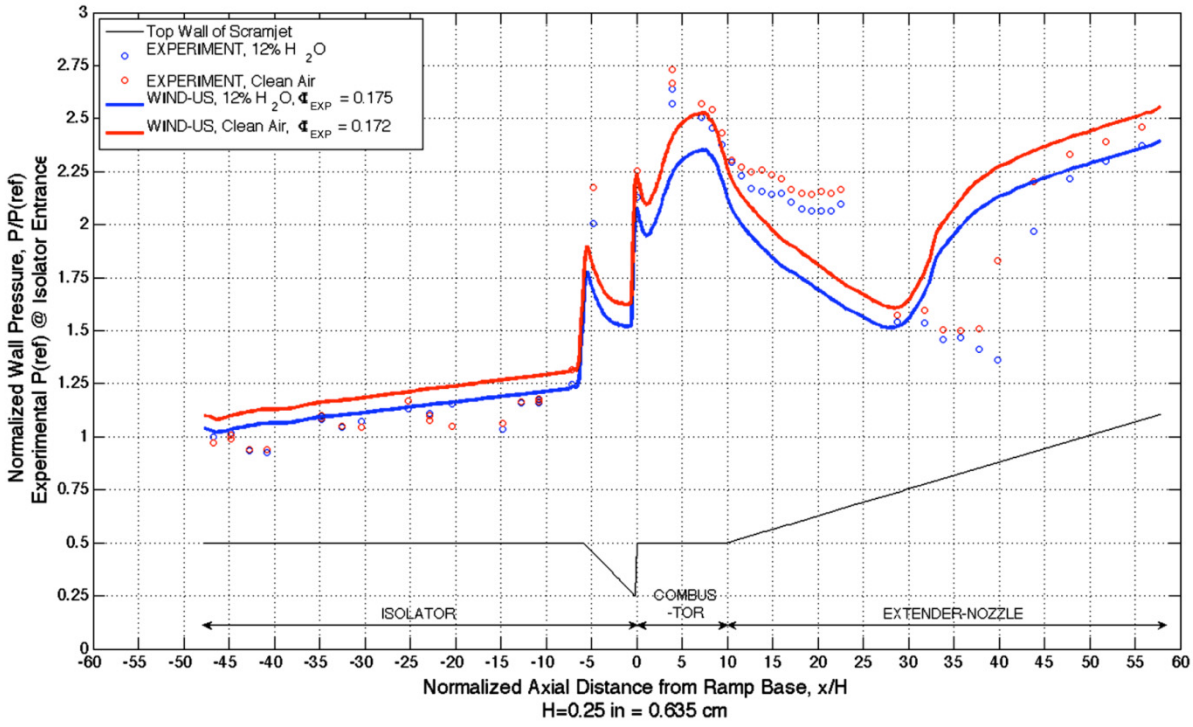

Figure 8.—Pressure along the fuel injector wall at symmetry plane, $\Phi_{EXP} \approx 0.170$.

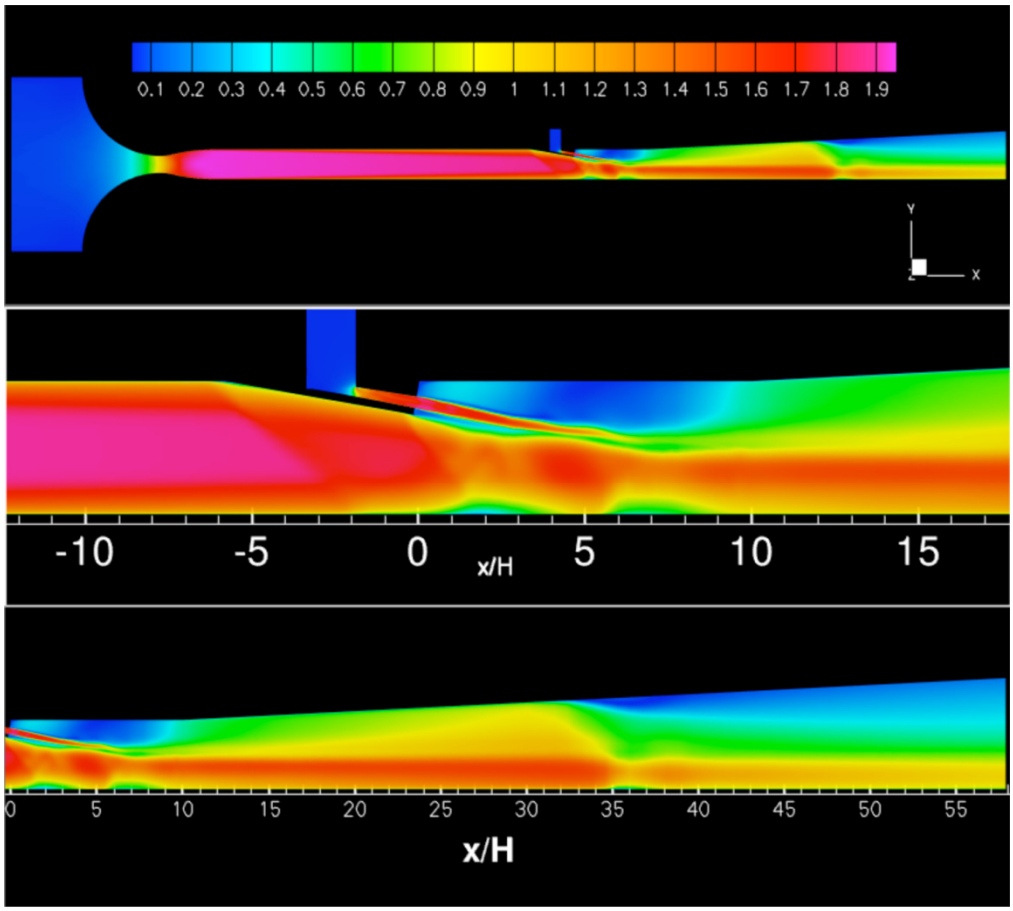

Figure 9.—Mach number contours at the symmetry plane, Φ_{EXP} = 0.172 (clean air).

C. $\Phi_{EXP} \approx 0.260$

Figure 10 shows an important result illustrating the effects of the flow vitiates on the combustion process and overall qualitative behavior of a dual-mode combustor. The numerical result and the experimental data presented for the clean air case demonstrate the high peak pressure in the combustor which results in the upstream movement of the shock train with an established leading edge at x/H = –22. The flow decelerates moving through a series of lambda shocks that terminate in a normal shock. As a result a significant portion of the flow entering the combustor in Figure 11 is near sonic or subsonic. Experimental data and numerical results presented for the 12 percent H_2O vitiate show that the presence of flow vitiates results in a lowered peak combustor pressure. In fact, as seen in Figure 12 the decrease in combustor pressure results in the shock train being swallowed, thus the flow entering the combustor is supersonic. This was expected because the experiment showed a considerable hysteresis in the fuel equivalence ratio range of 0.220 to 0.260 (Ref. 24). It seems that the mode transition can happen in this range depending on the flow conditions that would trigger it. For the UVa experiments it was the change in the fuel-equivalence ratio. However, in practice it would be the changing flight conditions combined with fuel-equivalence ratios.

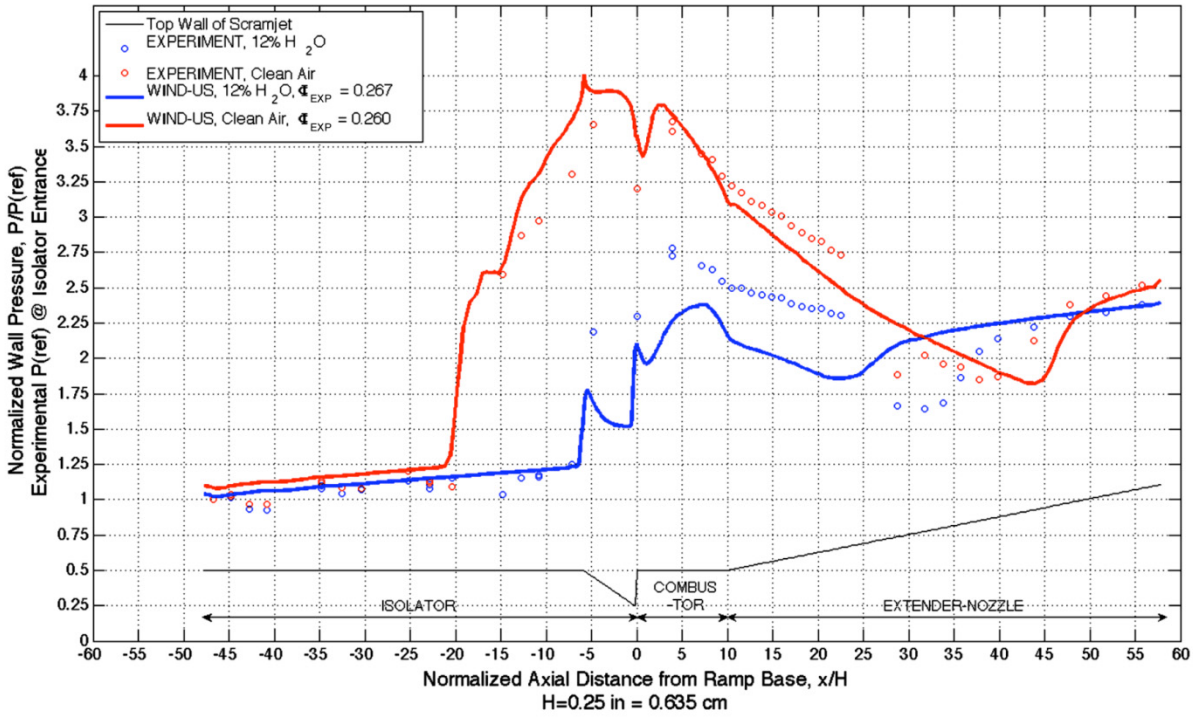

Figure 10.—Pressure along the fuel injector wall at symmetry plane, $\Phi_{EXP} \approx 0.260$.

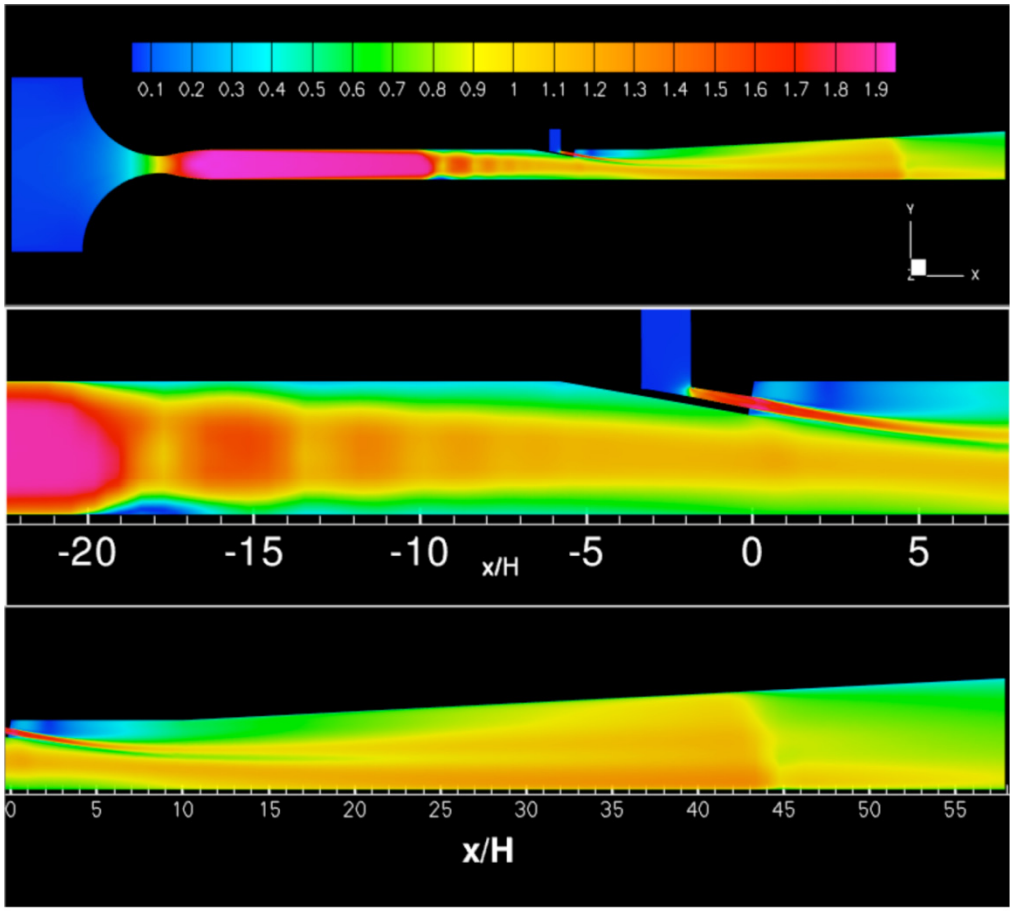

Figure 11.—Mach number contours at the symmetry plane, $\Phi_{EXP} = 0.260$ (clean air).

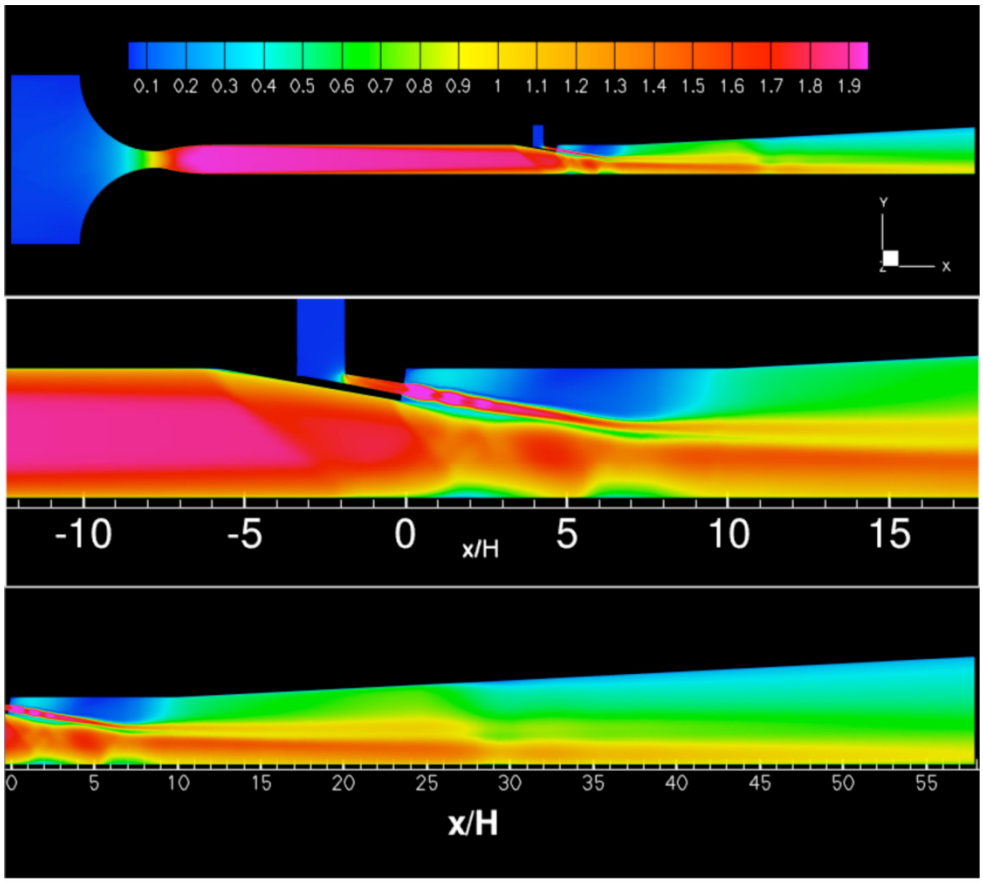

Figure 12.—Mach number contours at the symmetry plane, Φ_{EXP} = 0.267 (vitiated air).

The use of a constant Sc_t model gives an interesting result for both cases. The peak pressure in the combustor is over-predicted for the clean air case, thus the numerical result shows the leading edge of the shock train to be more forward than the experimental result. However, it provides a good match with experimental data in the extender-nozzle. In contrast, the peak pressure for the vitiated air case is under-predicted in the combustor and this discrepancy continues in the extender-nozzle as well.

From an evaluation of Figures 11 and 12, it is clear that the addition of H_2O vitiate to the supply nozzle airflow changed the operation of the combustor from subsonic to supersonic. A previous study was unable to capture this transition using a 1-reaction kinetics mechanism (Ref. 8). Figure 11 shows an upstream moving shock train due to relatively high combustor pressure. For clean air, the flow separation starts at x/H = –20 and gets thicker as the flow approaches the combustor entrance. The majority of the flow entering the combustor is subsonic, thus the combustor is operational in ramjet mode. However, with the addition of H_2O vitiate to the airflow, Figure 12 confirms an absence of the shock train. The compression ramp generates an initial shock that propagates downstream to the combustor. The majority of the flow entering the combustor is supersonic, thus the combustor is operational in scramjet mode.

D. $\Phi_{EXP} \approx 0.340$

Figure 13 shows a comparison of numerical results and the experimental data for clean and vitiated air cases at Φ_{EXP} = 0.341 and 0.349, respectively. The experimental data show a logical trend that is the addition of H_2O to the supply nozzle airflow reduces the overall pressures. The numerical results show a similar trend, however there is a subtle difference between the numerical results. They both show a good match to the peak pressure in the combustor and extender-nozzle. The leading edge of the shock train is accurately predicted for the clean air case at x/H = –26. But, the location of the leading edge of the shock

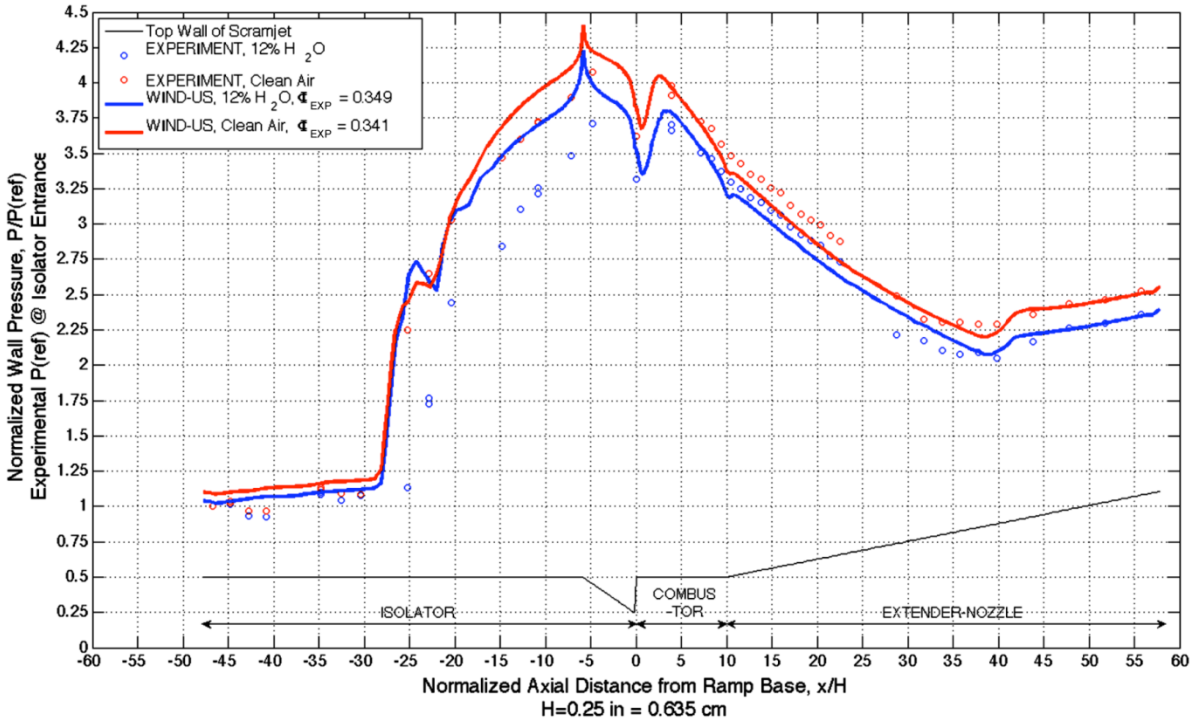

Figure 13.—Pressure along the fuel injector wall at symmetry plane, $\Phi_{EXP} \approx 0.340$.

train for the vitiated air case is more upstream than the experimental data. Moreover, the vitiated air case predicts combustor pressures relatively identical to that of the clean air case. This is likely due to the fact that the fuel-equivalence ratio for vitiated air is higher than for the clean air case. The pressures in the extender-nozzle look more reasonable for the vitiated air case when compared to the clean air result, i.e., lower pressures due to addition of flow vitiate.

It is important to mention that Sc_t was calibrated with the clean air case. This is likely the reason that the numerical simulation provides an excellent match to that of the experimental data for clean air. Figure 14 shows the Mach number contours for the clean air case. It is obvious that the high pressure in the combustor causes the shock train to move upstream. The shock wave boundary layer interactions cause a flow separation, which continues to grow through the isolator. As a result, the majority of the flow entering the combustor is subsonic, thus the combustor is operational in ramjet mode for both cases.

E. $\Phi_{EXP} \approx 0.460$

Figure 15 shows the comparison between numerical results and experimental data for clean and vitiated air cases at $\Phi_{EXP} = 0.454$ and 0.460, respectively. As expected, the experimental values of the overall pressure for clean air case are higher than the vitiated air case. A similar qualitative trend is observed in the numerical results as well. The clean air result shows a good overall match with the data in the combustor and extender-nozzle, but predicts the leading edge of the shock train upstream from where the data suggest. This could be due to the fact that the peak pressure is over-predicted, which forces the shock train upstream.

The vitiated air results show an excellent agreement with data in the isolator, combustor, and extender nozzle. The leading edge of the shock train is accurately predicted along with the peak pressure in the combustor. With the majority of flow entering the combustor being subsonic, the combustor operation is in ramjet mode for both cases.

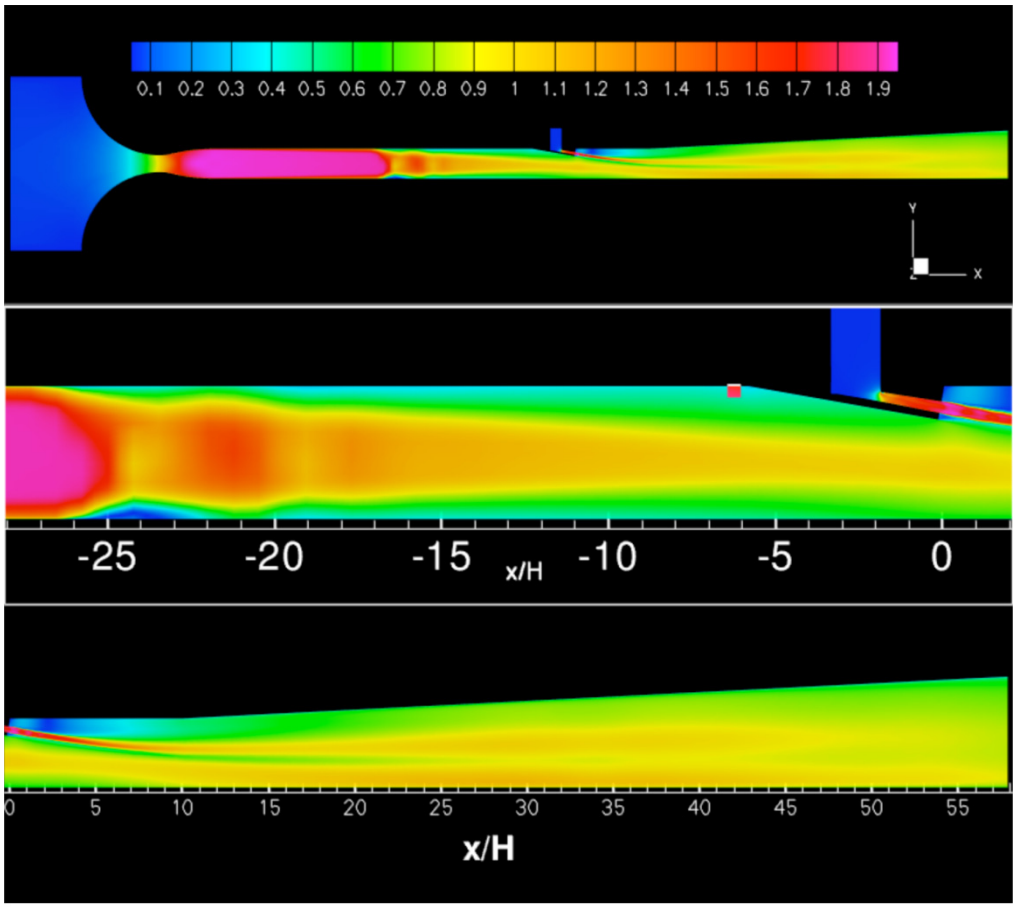

Figure 14.—Mach number contours at the symmetry plane, Φ_{EXP} = 0.341 (clean air).

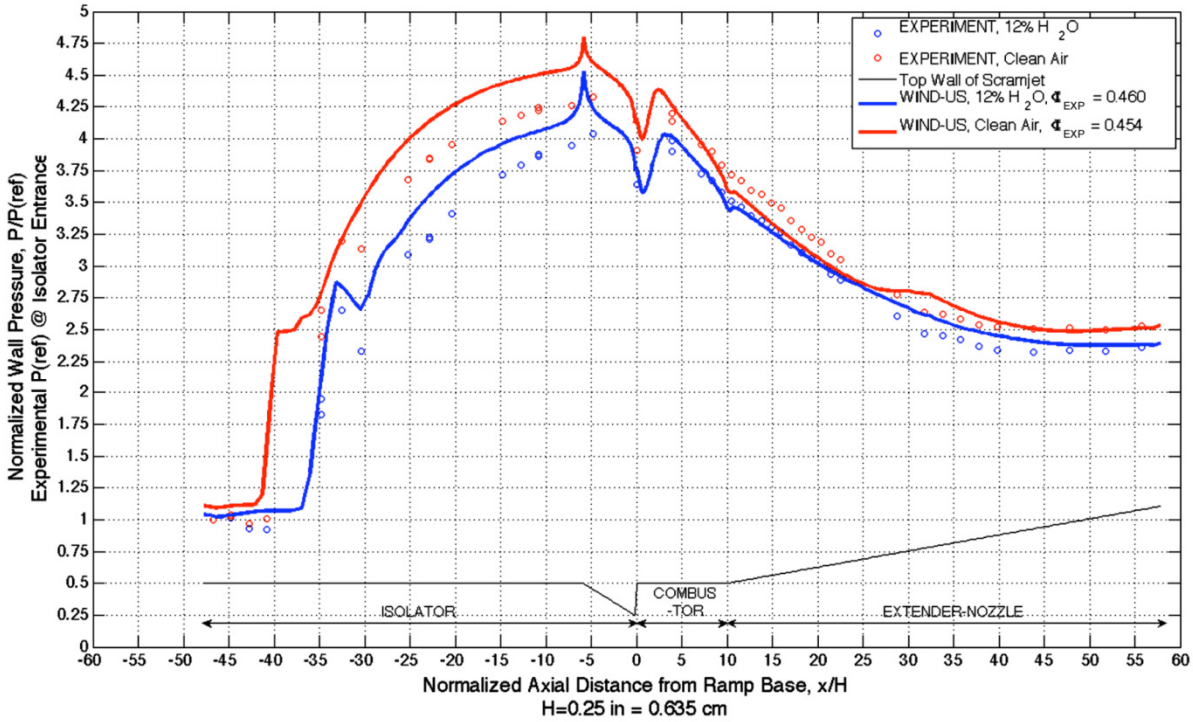

Figure 15.—Pressure along the fuel injector wall at symmetry plane, $\Phi_{EXP} \approx 0.460$.

F. Results Summary

Figures 16 and 17 show a summary of all clean and vitiated air simulations compared with the experimental data. The investigation shows a good qualitative match to the data. For the choice of baseline $Sc_t = 0.6$, the high fuel-equivalence ratios ($\Phi_{EXP} = 0.260$ to 0.460) provided a good quantitative match with experimental data in the isolator, combustor and extender-nozzle. However, for the low fuel-equivalence ratio ($\Phi_{EXP} = 0.172$, 0.175) a discrepancy was observed in the combustor and extender nozzle. Especially in the flowpath from x/H = 10 to 27, where the pressures are under-predicted and the simulation was unable to capture the steep decrease in pressure at x/H = 25. This was likely due to the fact that the Sc_t was calibrated for the higher fuel-equivalence ratios. The fuel-air mixing behavior that a constant Sc_t provides for a high fuel-equivalence ratio is significantly different than a low fuel-equivalence ratio. A variable Sc_t model is highly desirable and may also account for turbulence-chemistry interactions, which play a key role in fuel-air mixing and thus the combustion process. The results also showed that the mode transition happened in the fuel-equivalence range of 0.172 to 0.260.

The flow vitiation effects on the operation of a dual-mode combustor are also demonstrated in Figure 17. Especially for $\Phi_{EXP} = 0.267$ (compare to $\Phi_{EXP} = 0.260$), where the addition of flow vitiates effectively changed the operation of combustor from ramjet to scramjet mode. This is a key finding of this work. As discussed earlier, this result should also help researchers conducting experiments in large experimental facilities where fuel is burned to match the flight enthalpies, which inadvertently adds flow vitiates to the airflow. Similar to the clean air results, the fuel-equivalence ratios which demonstrated the scramjet mode showed a poor agreement with pressure in flowpath from x/H = 10 to 27. Overall, the pressures in the vitiated air cases were comparatively lower than the clean air counterparts.

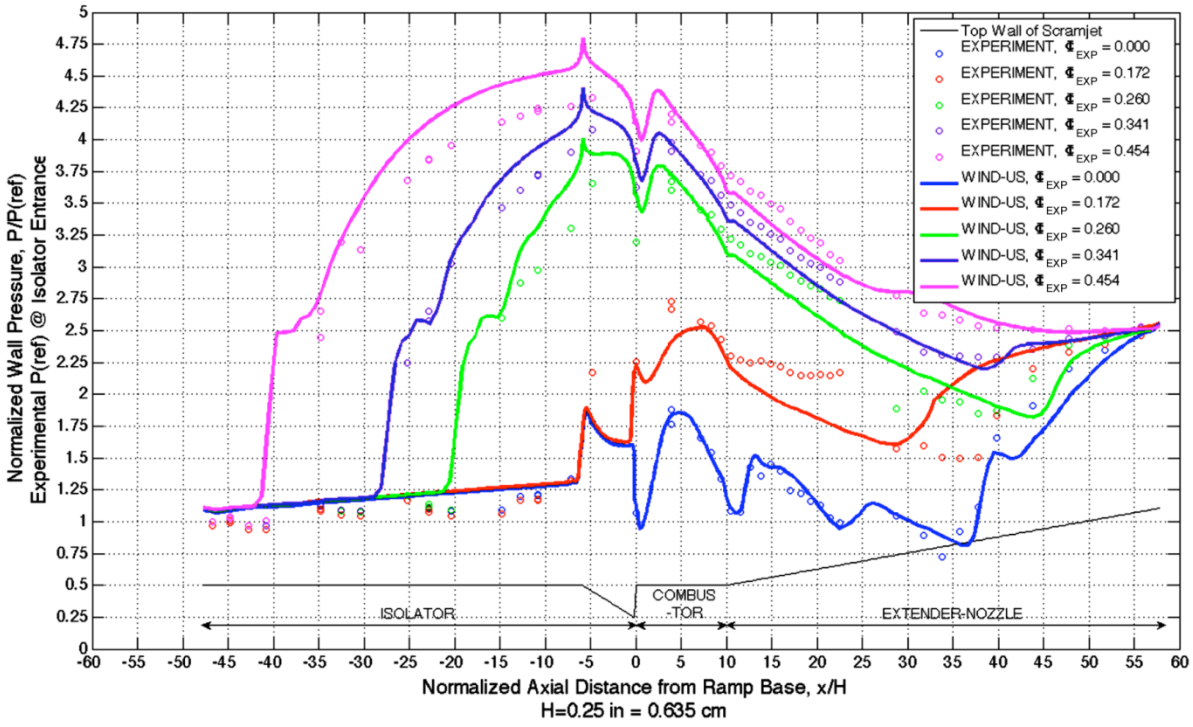

Figure 16.—Pressure along the fuel injector wall at symmetry plane, clean air.

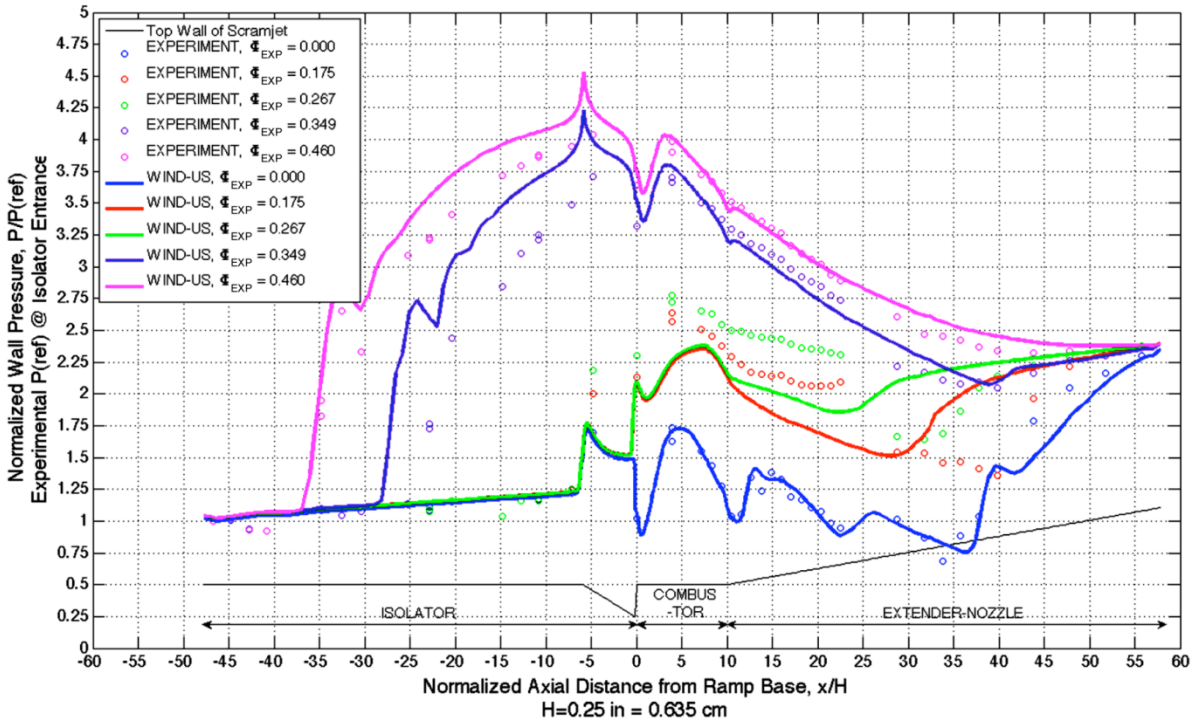

Figure 17.—Pressure along the fuel injector wall at symmetry plane, vitiated air.

VI. Conclusions

Wind-US was successfully utilized to perform numerical simulations of mode transition and investigate the effect of flow vitiation on the mode transition process. A range of fuel-equivalence ratios is examined for clean as well as vitiated air. A choice of HLLC numerical scheme, k-ε turbulence model, and 9-species, 18-reaction Peters and Rogg chemical kinetics model provided a good agreement with experimental data. A baseline constant Sc_t of 0.6 and Pr_t of 0.9 were utilized for all simulations.

The low fuel-equivalence ratio cases under-predicted the pressures in the combustor and extender-nozzle. This is attributed to the choice of a constant Sc_t and possibly the wall temperature boundary conditions. The discrepancy in the pressures at x/H = 25 was still unresolved at the time of this publication. The $\Phi_{EXP} = 0.267$ case showed a clear effect of flow vitiation on the combustion process, namely that the addition of flow vitiates changed the combustor operation from ramjet to scramjet mode. The high fuel-equivalence ratio cases provided a good match with experimental data in the combustor and extender-nozzle, however the pressures in the isolator were slightly over-predicted for the vitiated air cases.

Lastly, the temperature boundary condition plays a key role in such scramjet simulations. As discussed earlier, the complex nature of the UVa facility presents a challenge from the numerical simulation point-of-view. Even though care was taken to pick temperature boundary conditions that were representative of the actual facility, they could be improved, especially in the combustor and extender-nozzle. More temperature thermocouple data would be required to facilitate a more realistic representation of the thermal boundary conditions using the multiple boundary temperature specification capability of Wind-US.

References

1. Towne, C.E., "Wind-US Users Guide, Version 2.0," NASA/TM—2009-215804, 2009.
2. Lankford, D.W., Mani, M., "Wind Thermochemical Models and Recent Improvements," AIAA–2003–545, 2003.
3. Baurle, R.A., Eklund, D.R., "Analysis of Dual-Mode Hydrocarbon Scramjet Operation at Mach 4 – 6.5," AIAA–2001–3299, 2001.
4. Goyne, C.P., Rodriguez, C.G., Krauss, R.H., McDaniel, J.C., McClinton, C.R., "Experimental and Numerical Study of a Dual-Mode Scramjet Combustor," *Journal of Propulsion and Power*, Vol. 22, No. 3, 2006.
5. Engblom, W.A., Frate, F.C., Nelson, C.C., "Progress in Validation of WIND-US for Ramjet/Scramjet Combustion," AIAA Paper 2005-1000, 2005.
6. Bhagwandin, V.A., Engblom, W.A., Georgiadis, N.J., "Numerical Simulation of Hydrogen-Fueled Dual-Mode Scramjet Engine Using Wind-US," AIAA–2009–5382, 2009.
7. Heiser, W.H., Pratt, D.T., Hypersonic Airbreathing Propulsion, AIAA Education Series, Washington DC, 1994.
8. Sullins, G.A., "Demonstration of Mode Transition in a Scramjet Combustor," *Journal of Propulsion and Power*, Vol. 9, No. 4, 1993.
9. Georgiadis, N.J., Yoder, D.A., Towne, C.E., Engblom, W.A., Bhagwandin, V.A., Power, G.D., Lankford, D.W., Nelson, C.C., "Wind-US Code Physical Modeling Improvements to Complement Hypersonic Testing and Evaluation," AIAA–2009–193, 2009.
10. Evans, J.S., Schexnayder, C.J., "Influence of Chemical Kinetics and Unmixedness on Burning in Supersonic Hydrogen Flames," *AIAA Journal*, Vol. 18, No. 2, 1979.
11. Peters, N., and Rogg, B., Reduced Kinetic Mechanisms for Applications in Combustion Systems, Springer-Verlag, Berlin-Heidelberg, 1993.
12. Turns, S.R., An Introduction to Combustion, McGraw-Hill, USA, 2000.
13. Keistler, P.G., Hassan, H.A., Xiao, X., "Role of Chemistry/Turbulence Interaction in 3-D Supersonic Combustion," AIAA–2008–89, 2008.
14. Martin, M.P., "Exploratory Studies of Turbulence/Chemistry Interaction in Hypersonic Flows," AIAA–2003–4055, 2003.
15. Narayana, J.R., "Effect of Turbulence-Chemistry Interactions in Compressible Reacting Flows," AIAA–94–2311, 1994.
16. Xiao, X., Hassan, H.A., Baurle, R.A., "Modeling Scramjet Flows with Variable Turbulent Prandtl and Schmidt Numbers," *AIAA Journal*, Vol. 45, No. 6, 2007.
17. Goyne, C.P., Rockwel, R., Personal Communication with UVa.
18. Josyula, E., Gaitonde, D., Shang, J., "Nonequilibrium Hypersonic Flow Solutions Using the Roe Flux-Difference Split Scheme," AIAA–91–1700, 1991.
19. Nichols, R.H., Tramel, R.W., Buning, P.G., "Evaluation of Two High Orger WENO Schemes," AIAA–2007–3920, 2007.
20. Yoder, D.A., Georgiadis, N.J., "Implementation and Validation of the Chien K-Epsilon Turbulence Model in the WIND Navier-Stokes Code," AIAA–1999–745, 1999.
21. Menter, F.R., "Two-Equation Eddy-Viscosity Turbulence Models For Engineering Applications," *AIAA Journal* 0001-1452 Vol. 32, No. 8 (1598–1605), 1994.
22. Rodi, W., and Scheuerer, G. "Scrutinizing the k-ε Turbulence Model Under Adverse Pressure Gradient Conditions," *Transactions of the ASME Journal of Fluids Engineering*, Vol. 108, pp. 174–179.
23. Burrows, M.C., Kurkov, A.P., "Analytical and Experimental Study of Supersonic Combustion of Hydrogen in a Vitiated Airstream," NASA-TM-X-2828, 1973.
24. Rockwell, R., Goyne, C.P., "Experimental Study of Test Medium Vitiation Effects on Dual-Mode Scramjet Mode Transition," AIAA–2010–1126, 2010.

25. Anderson, J.D., Computational Fluid Dynamics, McGraw-Hill, Inc., 1995.
26. Anderson, J.D., Fundamentals of Aerodynamics, McGraw-Hill, Inc., 2001.
27. Anderson, J.D., Hypersonic and High Temperature Gas Dynamics, McGraw-Hill, Inc., New York, 1989.
28. Aung, K.T., "A Computational Study of Effects of Third-Body Efficiencies on Laminar Burning Velocities," AIAA–98–0806, 1998.
29. Billig, F.S., "Combustion Process in Supersonic Flow," *Journal of Propulsion and Power*, Vol. 4, No. 3, 1988.
30. Billig, F.S., "Research on Supersonic Combustion," *Journal of Propulsion and Power*, Vol. 9, No. 4, 1993.
31. Chelliah, H.K., Krauss, R.H., McDaniel, J.C., "Modeling of Vitiation Effects on H2-O2 Combustion Using Reduced Reaction Mechanisms," AIAA–94–2577, 1994.
32. Duan, L., Martin, M.P., "Effect of Finite-rate Chemical Reactions on Turbulence in Hypersonic Turbulent Boundary Layers," AIAA–2009–588, 2009.
33. Drummond, J.P., Rogers, R.C., Hussaini, M.Y., "A Detailed Numerical Model of a Supersonic Reacting Mixing Layer," AIAA–86–1427, 1986.
34. Forsythe, J.R., "Investigation of Modified Menter's Two-Equation Turbulence Models for Supersonic Applications," AIAA–99–0873, 1999.
35. Georgiadis, N.J., Rizzatta, D.P., Fureby, C., "Large-Eddy Simulation: Current Capabilities, Recommended Practices, and Future Research," AIAA–2009–948, 2009.
36. Jachimowski, C.J., "An Analysis of Combustion Studies in Shock Expansion Tunnels and Reflected Shock Tunnels," NASA/TP-3224, 1992.
37. Le, D.B., Goyne, C.P., Krauss, R.H., McDaniel, J.C., "Experimental Study of a Dual-Mode Scramjet Isolator," AIAA–2005–23, 2005.
38. Li, J., Ma, F., Yang, V., Lin, K.C., Jackson, T.A., "A Comprehensive Study of Combustion Oscillations in a Hydrocarbon-Fueled Scramjet Engine," AIAA–2007–836, 2007.
39. Norris, A.T., Chen, K-H, "Chemical Kinetics in the National Combustion Code," AIAA–2000–0334, 1998.
40. Riggins, D., Tackett, R., Taylor, T., "Thermodynamic Analysis of Dual-Mode Scramjet Engine Operation and Performance," AIAA–2006–8059, 2006.
41. Tiwari, S.N., Pidugu, S.B., "Role of H2-Air Chemistry Models in Reacting and Radiating Nozzle Flows," AIAA–2000–3595, 2000.
42. Williams, F.A., Combustion Theory, Perseus Books Publishing, Massachusetts, 1985.

REPORT DOCUMENTATION PAGE			Form Approved OMB No. 0704-0188

1. REPORT DATE *(DD-MM-YYYY)*	2. REPORT TYPE	3. DATES COVERED *(From - To)*
01-07-2010	Technical Memorandum	

4. TITLE AND SUBTITLE
Numerical Simulation of Vitiation Effects on a Hydrogen-Fueled Dual-Mode Scramjet

5a. CONTRACT NUMBER

5b. GRANT NUMBER

5c. PROGRAM ELEMENT NUMBER

6. AUTHOR(S)
Vyas, Manan, A.; Engblom, William, A.; Georgiadis, Nicholas, J.; Trefny, Charles, J.; Bhagwandin, Vishal, A.

5d. PROJECT NUMBER

5e. TASK NUMBER

5f. WORK UNIT NUMBER
WBS 031102.02.030738.09

7. PERFORMING ORGANIZATION NAME(S) AND ADDRESS(ES)
National Aeronautics and Space Administration
John H. Glenn Research Center at Lewis Field
Cleveland, Ohio 44135-3191

8. PERFORMING ORGANIZATION REPORT NUMBER
E-17332

9. SPONSORING/MONITORING AGENCY NAME(S) AND ADDRESS(ES)
National Aeronautics and Space Administration
Washington, DC 20546-0001

10. SPONSORING/MONITOR'S ACRONYM(S)
NASA

11. SPONSORING/MONITORING REPORT NUMBER
NASA/TM-2010-216756

12. DISTRIBUTION/AVAILABILITY STATEMENT
Unclassified-Unlimited
Subject Categories: 01, 02, and 07
Available electronically at http://gltrs.grc.nasa.gov
This publication is available from the NASA Center for AeroSpace Information, 443-757-5802

13. SUPPLEMENTARY NOTES

14. ABSTRACT
The Wind-US computational fluid dynamics (CFD) flow solver was used to simulate dual-mode direct-connect ramjet/scramjet engine flowpath tests conducted in the University of Virginia (UVa) Supersonic Combustion Facility (SCF). The objective was to develop a computational capability within Wind-US to aid current hypersonic research and provide insight to flow as well as chemistry details that are not resolved by instruments available. Computational results are compared with experimental data to validate the accuracy of the numerical modeling. These results include two fuel-off non-reacting and eight fuel-on reacting cases with different equivalence ratios, split between one set with a clean (non-vitiated) air supply and the other set with a vitiated air supply (12 percent H_2O vapor). The Peters and Rogg hydrogen-air chemical kinetics model was selected for the scramjet simulations. A limited sensitivity study was done to investigate the choice of turbulence model and inviscid flux scheme and led to the selection of the k-ε model and Harten, Lax and van Leer (for contact waves) (HLLC) scheme for general use. Simulation results show reasonably good agreement with experimental data and the overall vitiation effects were captured.

15. SUBJECT TERMS
Scramjet; Mode transition; Vitiated air; Equivalence ratio; Schmidt number

16. SECURITY CLASSIFICATION OF:			17. LIMITATION OF ABSTRACT	18. NUMBER OF PAGES	19a. NAME OF RESPONSIBLE PERSON
a. REPORT	b. ABSTRACT	c. THIS PAGE			STI Help Desk (email:help@sti.nasa.gov)
U	U	U	UU	28	19b. TELEPHONE NUMBER *(include area code)* 443-757-5802